Int J Legal Med (2018) 132:249–262
DOI 10.1007/s00414-017-1652-0

ORIGINAL ARTICLE

The role of angiography in the congruence of cardiovascular measurements between autopsy and postmortem imaging

Renaud Troxler[1] · Costin Minoiu[2] · Paul Vaucher[1,3] · Katarzyna Michaud[1] · Francesco Doenz[4] · Kewin Ducrot[1] · Silke Grabherr[1]

Received: 10 January 2017 / Accepted: 12 July 2017 / Published online: 24 July 2017

Abstract
Introduction Postmortem CT angiography is the method of choice for the postmortem imaging investigations of the cardiovascular (CV) system. However, autopsy still remains the gold standard for CV measurement. Nevertheless, there are not any studies on CV measurements on the multi-phase postmortem angiography (MPMCTA) which includes comparisons with autopsy. Therefore, the aim of this study is to compare CV measurements between the native CT scan and the three phases of the MPMCTA to find out which of these modalities correlate the best with autopsy measurements.
Methods For this study, we selected retrospectively 50 postmortem cases that underwent both MPMCTA and autopsy. A comparison was carried out between the CV measurements obtained with imaging (*aorta*; *heart cavities and cardiac wall thicknesses*; *maximum cardiac diameter* and *cardiothoracic ratio*) and at the autopsy (*aorta*; *cardiac valves*, *ventricular thicknesses*, and *weight*).
Results Our results show that the dynamic phase displays an advantage for the measurement of the aortas. However, the MPMCTA is not accurate to measure the cardiac wall thicknesses. The measurements of the heart cavities show no correlation with the heart valves. The cardiothoracic ratio measured by the MPMCTA shows no correlation with the heart weight. Nevertheless, the maximum cardiac diameter exhibits a correlation with the latter on the venous and dynamic phase.
Conclusions These results show that only few CV parameters measured with imaging correlate with measurement obtained at the autopsy. These results indicate that in order to better estimate values obtained at the autopsy, we need to define new reference values for the CV measurement on MPMCTA.

Keywords Forensic imaging · MPMCTA · Cardiovascular measurement · Autopsy

Introduction

The postmortem CT angiography (PMCTA) is the method of choice for the postmortem (PM) imaging investigations of the cardiovascular (CV) system [1–4]. It is actually performed in a series of forensic medical centers around the world [4–6]. The PMCTA can be performed on single organs [6, 7] or on the whole body [1, 4, 8–11]. The first one consists in injecting a targeted organ in situ or after its extraction from the body [8]. The second one is a CT angiography that visualizes the whole CV system [5]. It is more useful in detecting vascular abnormalities [4, 6, 9, 11], which cannot be seen with a conventional autopsy.

The standardized protocol developed by Grabherr et al. allows PMCTA of great qualities [12] with three angiographic phases [12]: the multi-phase postmortem CT angiography (MPMCTA). This latter allows a good opacification and

Electronic supplementary material The online version of this article (doi:10.1007/s00414-017-1652-0) contains supplementary material, which is available to authorized users.

✉ Silke Grabherr
Silke.Grabherr@chuv.ch

[1] University Center of Legal Medicine Lausanne-Geneva, Chemin de la Vulliette 4, 1000, 25 Lausanne, Switzerland

[2] University of Medicine and Pharmacy "Carol Davila", Bucharest, Romania

[3] School of Health Sciences Fribourg, University of Applied Sciences and Arts Western Switzerland (HES-SO), Rue des Cliniques 15, 1700 Fribourg, Switzerland

[4] Department of Diagnostic and Interventional Radiology, University Hospital of Lausanne, Lausanne, Switzerland

visualization of the CV system. Some studies compare the MPMCTA with the autopsy findings [3, 5, 12, 13] in order to implant imaging as an accurate tool to determine the cause of death. Furthermore, MPMCTA is the method of choice to visualize vascular abnormalities, such as vessel dissection, aneurism, and occlusion. All these indications [1–5, 9, 11–13] make the MPMCTA one of the best techniques to investigate the CV system.

According to the textbooks and recommendations set in the field of the cardiovascular pathology, the standard gross examination of the heart includes the following measurements: heart weight, free wall thickness of the left ventricle, right ventricle, and of the septum, as well the circumference of valve rings [14–16]. The postmortem assessment of the aorta comprises the measurements of the wall circumference at various levels.

These measurements have to be compared with reference values and are ones of the key pieces of information used to help determine if cardiovascular pathology exists. It is therefore essential to find radiological measurements thanks to MPMCTA that correlate to the ones obtained at autopsy. Furthermore, the clinical radiologic parameters could not simply be applied because in postmortem imaging, there are other reference values [17–21].

However, to our knowledge, there are not any studies on the CV measurements on MPMCTA which includes comparisons with autopsy finding, although CV measurements on native postmortem CT scan already exist in some studies [17–24].

Therefore, the aim of this present study is to compare some CV measurements between the native CT scan and the three phases of the MPMCTA to find which of these four methods correlate the best with the autopsy measurements.

Methods and materials

The following study was approved by the Cantonal Ethics Committees on research involving humans (CER-VD; No. 130/15).

Subjects

Fifty postmortem cases investigated between October 2013 and June 2014 in the University Center of Legal Medicine in Lausanne were retrospectively included in this study. The inclusion criteria were all cases that underwent a native CT scan followed by MPMCTA and a medico-legal autopsy. The exclusion criteria were the following: cases with prosthetic valve or pacemaker, polytrauma cases, and cases with a dissection of the thoracic aorta associated with a cardiac tamponade. The latter did not permit accurate CV measurements.

Radiological investigations

A native CT scan of the corpse in supine position with the arms crossing with each other on the abdomen, from the skull vertex to the pelvis (genitals included), was performed before any manipulation. The scans were done using a General Electric (GE) Lightspeed 8-slice CT scanner (GE Healthcare, Milwaukee, WI, USA), using the parameters exposed in Table 1.

Then, an external examination was performed before the MPMCTA. The latter was carried out according to the protocol developed by Grabherr et al. [12]. MPMCTA is performed by injecting a mixture of 3.5 l of paraffin oil and contrast agent 6% (210 ml of Angiofil ®) (Angiofil®, Fumedica AG, Muri, Switzerland) [12, 25] through a modified heart-lung machine, Virtangio® perfusion device (Virtangio®, Fumedica AG, Maquet®, Muri, Switzerland), to reproduce a flow within the body's vascular system. Firstly, the "arterial phase" consists of filling, via the femoral artery, the arterial vascular system with 1200 ml of a mixture made of paraffin oil with contrast agent. This allows the visualization of the arterial bed with the CT scan. Then, the "venous phase" consists of filling, via the femoral vein, the venous vascular system with 1800 ml of the mixture. Finally, the "dynamic phase" is an acquisition of CT scan imaging while injecting additional 500 ml of the mixture in the arterial vascular system and an autonomously backflow from the femoral vein. Thanks to this synchronization of contrast agent perfusion with imaging acquisition, the CV system can be visualized as in vivo on the dynamic phase. MPMCTA included three CT scan (arterial, venous, and dynamic) phases of the body in the same position as the native CT scan, from the skull vertex to the knees, with the same device used for the native CT scan but with different parameters (Table 1).

Radiological measurements

A team of two board-certified radiologists decided upon common agreement on the location where each of the CV measurements should be performed. The CT measurements were carried out using a market-available software (Advantage Window–GE, AW Server 2.0) (GE Healthcare, Milwaukee, WI, USA). Then, all the measurements were made by a medical student, who was trained by the two radiologists, using the mediastinal or bone window, using always the same level for the same anatomical structure, in the four phases of the MPMCTA (native, arterial, venous, and dynamic), for each of the cases in order to permit an accurate comparison. Each of the measurements were reviewed and confirmed during a second view by a board-certified radiologist.

The diameter of the descending aorta was measured in an axial view at the level of the emergence of the right pulmonary artery (Fig. 1). The abdominal aorta was measured in an axial

Table 1 CT scan parameters

	Native CT scan				MPMCTA		
	Head	Head and cervical spine	Thorax and abdomen	Lower limbs[a]	Arterial phase	Venous phase	Dynamic phase
Localization	From the vertex to the base of the skull	From the vertex to D1	From the shoulders (included) to the pelvis (genitals included)	From the acetabulum (included) to the toes (included)	From the vertex to the pelvis	From the vertex to the pelvis	From the vertex to the pelvis
Scan type (s)	Axial full 1.0	Helical full 1.0	Helical full 1.0	Helical full 1.0	Helical full 1.0	Helical full 1.0	Helical full 1.0
Field of view (cm)	25	25	50	50	50	50	50
Slice thickness (mm)	5; interval 20 mm	1.25; spaced every 1 mm	1.25; spaced every 1 mm	1.25; spaced every 1 mm	1.25; spaced every 0.6 mm	1.25; spaced every 1.2 mm	2.25; spaced every 2 mm
Voltage (kV)	120	120	120	120	120	120	120
Dose (mA)/modulation index	300	100–350/15.00	100–350/15.00	100–350/15.00	300	300	300
Reconstruction algorithm	Standard	Standard Bone reconstruction	Standard Bone reconstruction Lung reconstruction (only on the lungs)	Standard Bone reconstruction	Standard	Standard	Standard

[a] If needed, in case of brunt body, multiple traumatic injuries, decomposed body

view, also on its minor axis, at the level of the departure of the renal arteries (Fig. 2). The method used to measure the descending and abdominal aorta were the same for the native CT scan and the three phases of the MPMCTA. Whenever situation was imposing, the diameter of the vessels was measured on their minor axis to avoid an overestimation. So, to illustrate that principle, comparisons are made between aorta and cylinders on a sectional view. If the latter is not exactly perpendicular, the cross-sectional area will be elliptical and will not allow an accurate measurement of the real diameter.

All cardiac measurements were carried out using a reformatted four-chamber view derived from the algorithm proposed by Lu et al. [26]. The method consists of creating a plane axe through the cardiac apex and the midpoint of the mitral valve using a sagittal view. On the reformatted four-chamber view, a scrolling was performed to find the two slices that permit the best visualization of the right and the left heart cavities, respectively.

On the slice depicting the left cardiac cavities, the left atrium and ventricle were measured, as well as the interventricular septum and left ventricular wall thicknesses (Fig. 3). The left atrium was measured on the minor axis from the left to the right inner walls. The left ventricle was measured midway between the mitral valve and the cardiac apex on the minor axis from the outer left ventricular wall and the inner right ventricular cavity.

The measurements of the right cardiac cavities were carried out similarly. On the slice that depicted the latter, the right atrium and ventricle were measured, as well as the right ventricular wall thickness (Fig. 4). The right atrium was measured on the minor axis from the left to the right inner walls. The right ventricle was measured midway between the tricuspid valve and the cardiac apex on the minor axis from the outer right ventricular wall and the inner right ventricular cavity. The methods to measure the heart cavities were identical for the three phases of the MPMCTA.

The cardiothoracic ratio (CTR) was measured according to the method proposed in the literature [21, 23] consisting of finding and measuring on an axial plane the maximum cardiac diameter from the right to the left. Then, the maximum thoracic diameter was measured on the same slice in a similar manner (Fig. 5). Thus, the CTR was calculated by dividing the maximum cardiac diameter with the maximum thoracic diameter.

Autopsy

Autopsies were performed in accordance with international guidelines [14, 27, 28] by two forensic pathologists (including at least one board-certified). During the procedure, CV measurements were collected as follows: descending and abdominal aorta circumferences were measured in the proximal part and at the level of the renal arteries, respectively. The left and right ventricular wall thicknesses were measured 1 cm below the cardiac valves on an axial slice, the same goes for the interventricular septum thickness. The circumferences of the

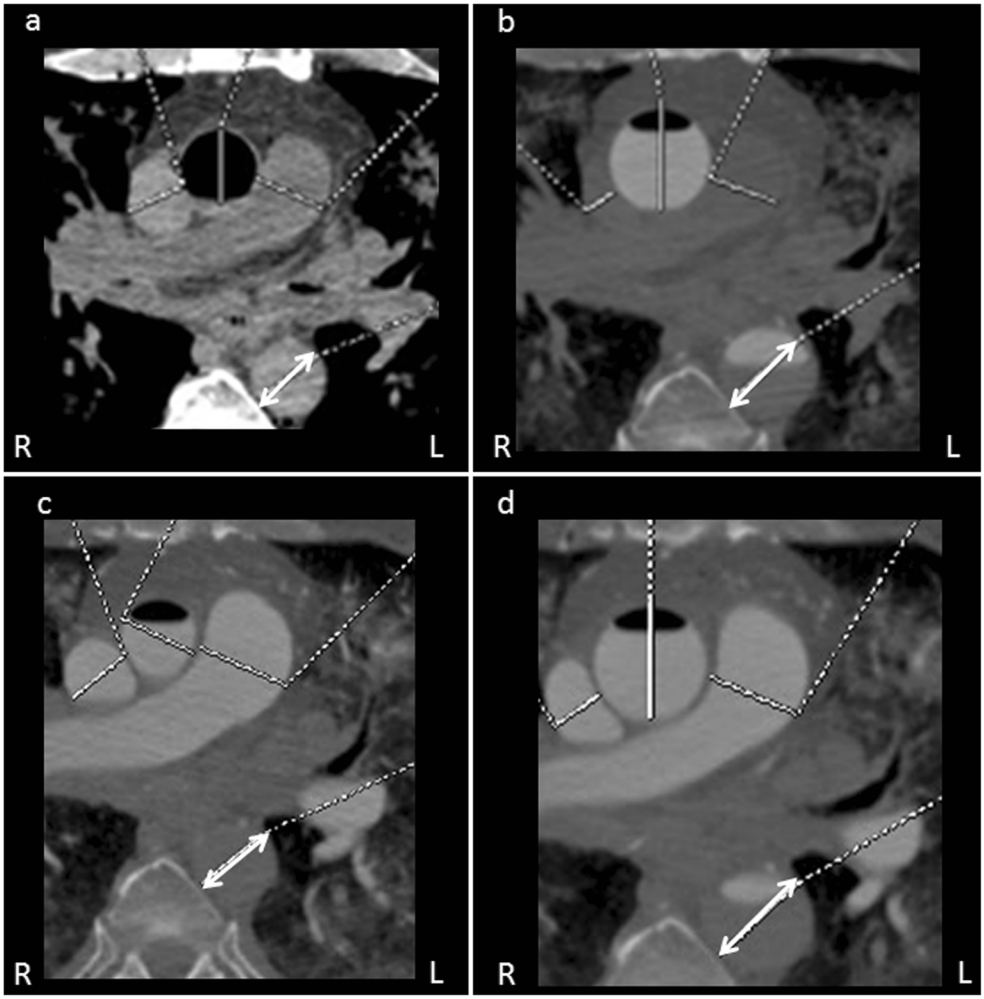

Fig. 1 Measurement of the descending aorta diameter (*white arrows*) on the minor axis in axial section. **a** Native CT scan. **b** Arterial phase. **c** Venous phase. **d** Dynamic phase. *R* right, *L* left

four cardiac valves (tricuspid, mitral, aortic, and pulmonary) were also measured. The emerging points of the great cardiac vessels were cut, and the heart (with epicardial fat) was excised. The hearts were emptied of postmortem clots and weighed [29] unfixed on a precision electronic balance (DIBAL HD-310; 0–15-kg range, 1-g intervals; Vizcaya, Spain).

Statistical methods

A convenient sample size of 50 cases was chosen. Parameters that were not measurable on CT-scans were identified and described. The prevalence and underlying patterns were described for each CT scan phase. The adjusted coefficient of determination (R^2) was measured to test the correlation between autopsy and radiological measurements using analysis of variance. Bland Altman analysis was used to verify homoscedasticity and standardized error between autopsy and CT scan. For the aorta, the minimal diameter was calculated from the circumference measured during the autopsy for comparability with radiological measurements. To test whether other phases than the dynamic phase were better at modelling true values measured at the autopsy, we used the Bayesian information criterion (BIC) to compare non-nested models (native CT scan, arterial phases, venous phase, and dynamic phase). We then used Raftery's rule [30] to define to what extend another phase was an improvement over the dynamic phase (0–2, weak; 2.1–6, positive; 6.1–10, strong; >10, very strong). All analyses were performed with STATA 12.0 (StataCorp LP, College Station, TX, USA).

Results

Population description

The population of the study was made of 50 medico-legal cases (Table 2). In 39 men (78%) and 11 women (22%) with a mean age of 58.2 (SD 18.3) and a mean body mass index (BMI) of 27.2 (SD 4.8), the causes and circumstances of death were the following: natural cardiac (n = 10); natural other (n = 10) including hemorrhage, pulmonary embolism, and

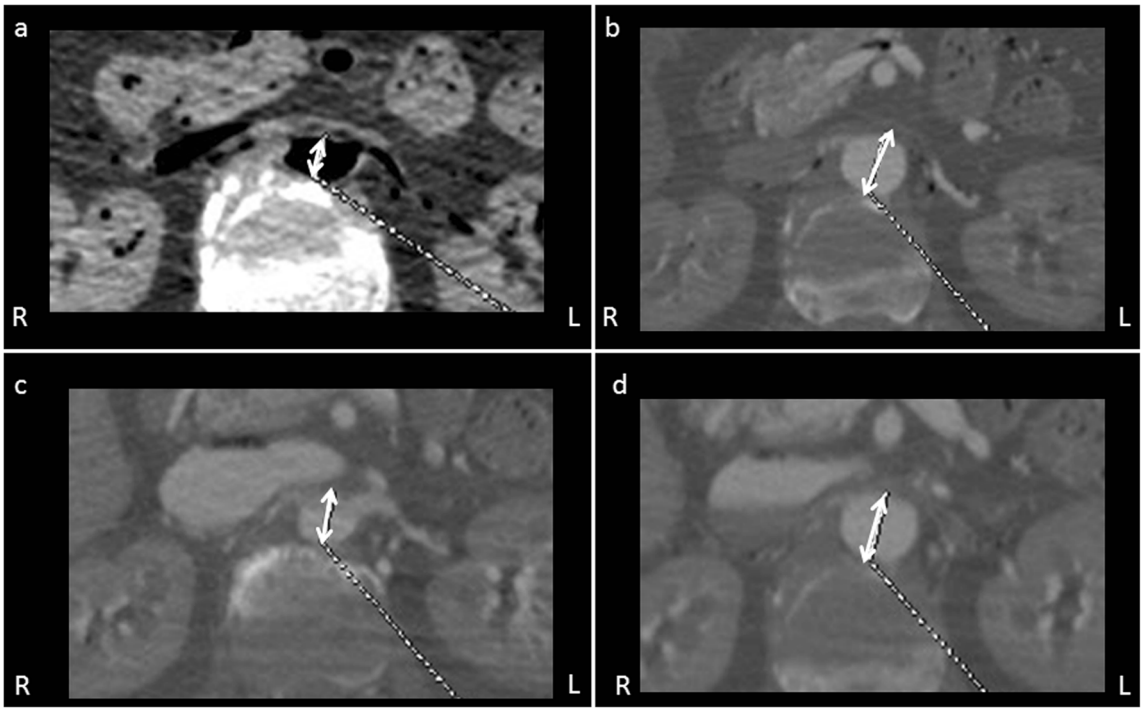

Fig. 2 Measurement of the abdominal aorta diameter (*white arrows*) on the minor axis in axial section. **a** Native CT scan. **b** Arterial phase. **c** Venous phase. **d** Dynamic phase. *R* right, *L* left

cerebral infarct; traumatic (n = 15); intoxication (n = 3); and other (n = 12) including asphyxia, multiple organ failure, medical errors, and unknown. The mean delays between death and MPMCTA and between MPMCTA and autopsy were 1.4 days (SD 0.7) and 0.6 days (SD 0.2), respectively.

Feasibility of assessment on CT scan

As the vascular system needs to be filled completely for the measurements and the vessels are filled in different phases, it was important to investigate which measurement could be obtained in which phase. Additionally, we had to verify if all measurements were feasible to be taken in all cases.

On the dynamic phases, the right ventricular wall thickness was always measurable. However, the measurements of the left ventricular wall and the interventricular thicknesses were impossible for seven and three cases, respectively. In cases where the measurements of the left ventricular wall thickness were not possible on the dynamic phase (n = 7), two cases were measurable on the venous phase. In the three cases where the interventricular septum thicknesses were not visible on the dynamic phase, one case was measurable on the venous phase. But in all cases, the unmeasurable thicknesses on the dynamic or venous phase were impossible on the arterial phase.

At least one of the thickness measurements (right or left ventricular wall and interventricular septum) was unrealizable on the arterial phase for 24 cases (48%). In comparison, on the dynamic phase, the latter were impossible only for seven cases (14%; Fisher's exact test $p < 0.001$).

With respect to the venous phase, the left ventricular wall thickness measurement was impossible for seven cases, but two cases were measurable on the dynamic phase. Regarding the interventricular septum thickness, three cases were unmeasurable on the venous phase; one of them became measurable on the dynamic phase. To summarize, the measurement should be carried out on priority on dynamic phase and if not feasible, on the venous phase.

Correlation of the descending and abdominal aorta between autopsy and imaging

The autopsies performed after the radiological examinations allow a direct comparison between diameters measured on the CT scan and the circumferences of the aortas at the dissection. Concerning the descending aorta, the different measurements are exposed in Table 3. A good correlation was obtained between the dynamic phase and the autopsy (R^2 = 0.382; $p < 0.001$) (Fig. 6). The BIC performed proved that the dynamic phase is the best to estimate the value measured at the autopsy (Table 4). The other phases of the MPMCTA and the native CT scan were less accurate to measure the real diameter of the aorta (native = 8.6; arterial = 13.2; venous = 3.9).

The measurement of the abdominal aorta, exposed in Table 3, showed similar results. The correlation between autopsy and dynamic phase was equally good (R^2 = 0.486; $p < 0.001$) (Fig. 6), and the BIC analyses displayed the great

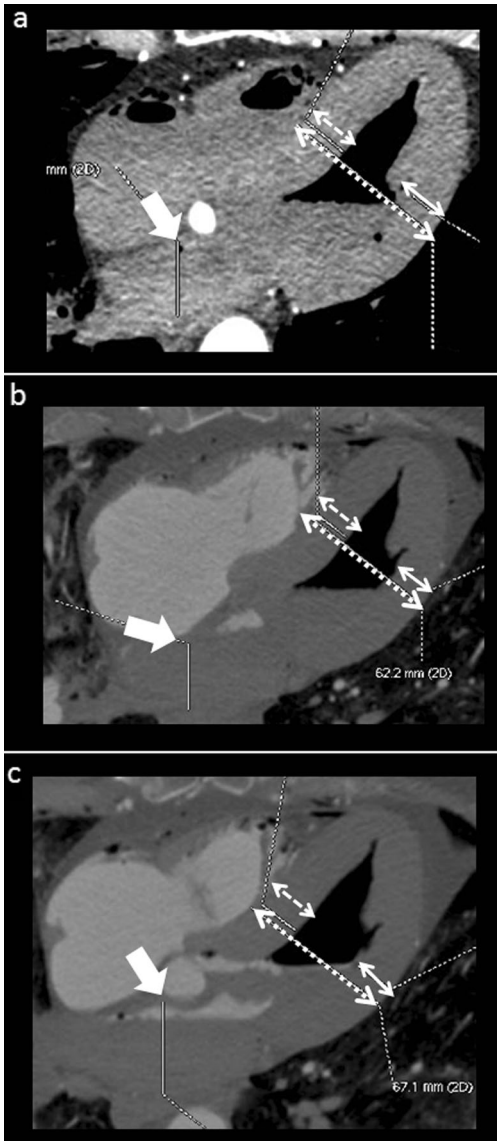

Fig. 3 Measurement of the left cardiac cavities with a reformatted four-chamber view in axial section. **a** Arterial phase. **b** Venous phase. **c** Dynamic phase. Visualization of the left atrium (*white arrowheads*), the left ventricle (*white dotted arrows*), the left ventricular wall thickness (*white arrows*), and the interventricular septum thickness (*white dotted line arrows*).

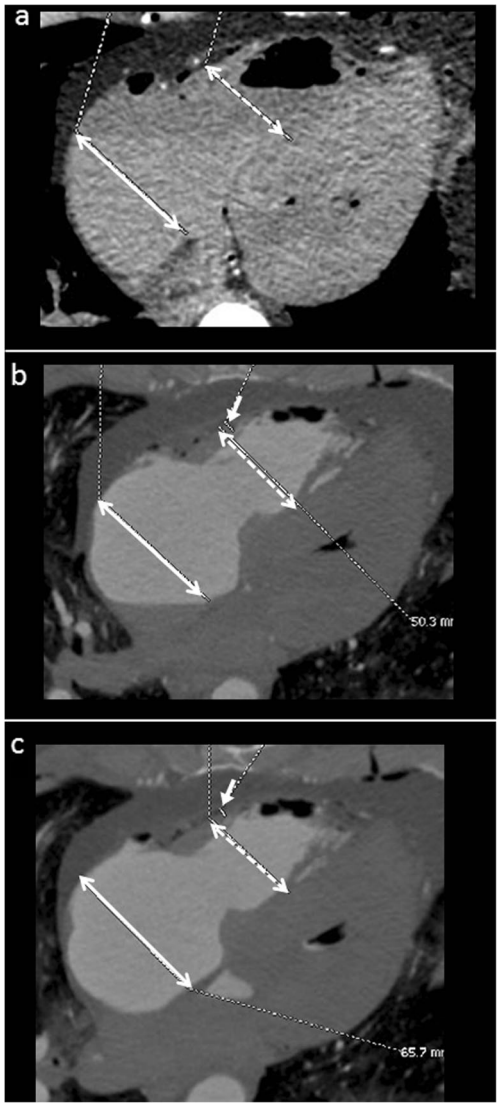

Fig. 4 Measurement of the right cardiac cavities with a reformatted four-chamber view in axial section. **a** Arterial phase. **b** Venous phase. **c** Dynamic phase. Visualization of the right atrium (*white arrows*), the right ventricle (*white dotted line arrows*), and the right ventricular wall thickness (*white arrowheads*).

advantages to perform the measurements on the dynamic phase (native = 19.2; arterial = 14.7; venous = 6.2) (Table 4).

Correlation of the cardiac thicknesses between autopsy and imaging

The measurements of the cardiac thicknesses (right and left ventricular wall and interventricular septum) were carried out at the autopsies, as well as the aorta diameters (Table 3). However, the measurements of the thicknesses displayed no correlation (Table 4). The R^2 calculated for the right, the left ventricular wall thicknesses, and the interventricular septum were 0.004, 0.07, and 0.087 (Fig. 6), respectively. Furthermore, the BIC performed did not display an advantage to measure the thickness on the dynamic phase for the three thicknesses (Table 4).

Bland Altman analysis comparing dynamic CT scan to autopsy findings shows contradictory results between left and right ventricular thickness making it difficult to interpret results and exclude random error. When comparing septum thickness, the error seems homoscedastic and centered on zero. Similar magnitudes of error were observed between CT scan phases, suggesting that errors might be due to lack of reliability in setup thickness on the CT scan (Fig. 7).

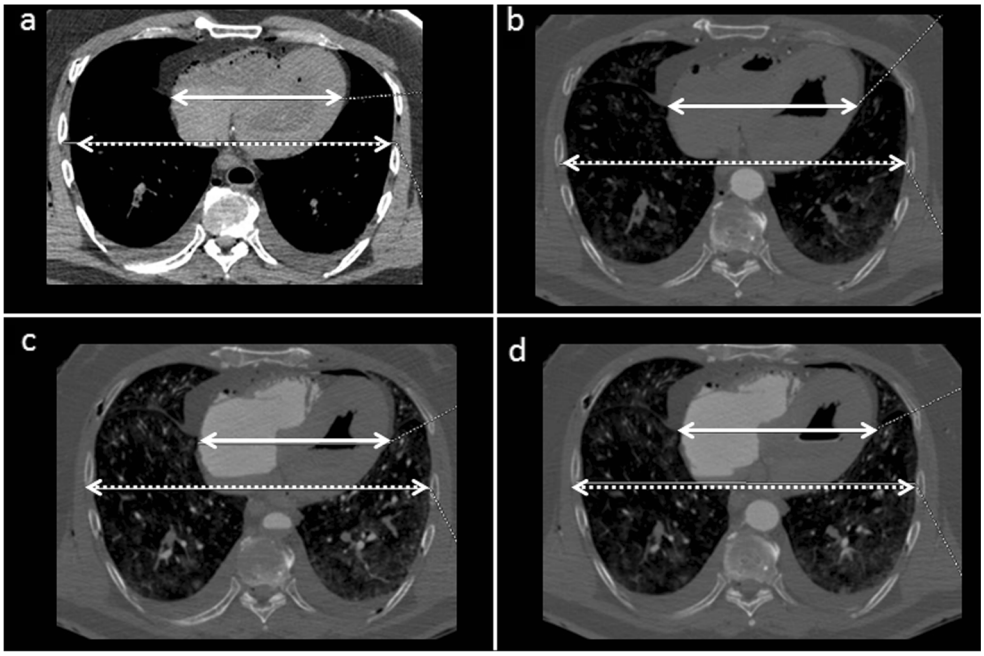

Fig. 5 Measurement of the cardiothoracic ratio with the maximum cardiac diameter (*white arrows*) and the maximum thoracic diameter (*white dotted arrows*) in axial section. **a** Native CT scan. **b** Arterial phase. **c** Venous phase. **d** Dynamic phase.

Correlation between the cardiac valves and heart cavities

We did not find any significant correlation between the right atrium and the tricuspid valve on the dynamic phase (R^2 = <0.001); the right ventricle and the pulmonary valve on the dynamic phase (R^2 = 0.027); the left atrium and the mitral valve on the dynamic phase (R^2 = <0.001); and the left ventricle and the aortic valve on the dynamic phase (R^2 = <0.001) (Table 5). Moreover, the BIC analyses did not display an advantage to make the measurement on any phases.

Table 2 Population description

Sample characteristics	%/Mean	*n*/SD
Number of case	–	(50)
Men	78%	(39)
Cause of death		
Natural cardiac	20%	(10)
Natural other	20%	(10)
Traumatic	30%	(15)
Intoxication	6%	(3)
Other	24%	(12)
Age	58.2	(18.3)
BMI	27.2	(4.8)
PM delay (day)		
Death to MPMCTA	1.4	(0.7)
MPMCTA to autopsy	0.6	(0.2)
Death to autopsy	2	(0.7)

Finally, the absence of association between the cardiac valves and heart cavities was not in connection with the PM delays or the causes of death.

Correlation between the heart weight and the CTR or the maximum cardiac diameter

There was no correlation between the CTR and the heart weight on the dynamic phase (Table 6) (R^2 = 0.075; $p < 0.05$). Furthermore, the BIC analyses did not point out any advantage to measure the CTR on one phase over another to get a good correlation with the heart weight.

Nevertheless, we found a significant correlation between the maximum cardiac diameter and the heart weight on the dynamic phase (Table 6) (R^2 = 0.418; $p < 0.001$) (Fig. 6). We found that

$$\textit{Dynamic phase} : \textit{heart weight}\ (\mathrm{g}) = \textit{heart width}\ (\mathrm{mm}) \times 6.1 - 397$$

$$\textit{Venous phase} : \textit{heart weight}\ (\mathrm{g}) = \textit{heart width}\ (\mathrm{mm}) \times 6.0 - 384$$

Blant Altmann analysis shows us that this formula tends to overestimate weight for light hearts (300 g) by about 75 g and overestimate weight of heavy hearts (700 g) by 100 g in a linear way.

The BIC analyses displayed the great advantage to make the measurement on the dynamic or the venous phase (BIC = −0.2), compared to the native CT scan (BIC = 11.9) and the arterial phase (BIC = 9.9).

Table 3 Cardiovascular measurements

	Native mean; SD; *n*	Arterial mean; SD; *n*	Venous mean; SD; *n*	Dynamic mean; SD; *n*	Autopsy mean; SD; *n*
Aortas (mm)					
Descending	18.8; (4.4); 50	25.1; (3.2); 50	20.8; (4.2); 50	24.3; (3.6); 50	18.8; (3.7); 50
Abdominal	9.2; (4.5); 50	17.6; (3.2); 50	14.3; (4.2); 50	18.1; (3.2); 50	14.7; (3.1); 50
Thicknesses (mm)					
Right ventricular wall	–	5.2; (1.8); 31	4.9; (1.9); 49	4.4; (1.7); 50	4; (1.8); 50
Left ventricular wall	–	14.5; (4); 34	15.3; (4.1); 43	15.2; (4.3); 43	13.8; (2.8); 50
Interventricular septum	–	14.6; (3.8); 38	12.6; (3.4); 47	13.5; (3.5); 47	13; (3.1); 50
Heart cavities (mm)					
Right ventricle	–	36.8; (9.2); 50	48.5; (10.7); 50	45.8; (10.4); 50	–
Left ventricle	–	56.6; (9.2); 50	51.6; (6.6); 50	54.6; (8.2); 50	–
Right atrium	–	51; (11.5); 50	60.6; (9.2); 50	59.4; (9.2); 50	–
Left atrium	–	28.3; (8.8); 50	30; (8.1); 49	32.1; (7.8); 49	–
Valves (mm)					
Mitral	–	–	–	–	10.(8; 1); 50
Tricuspid	–	–	–	–	12.5; (1.3); 50
Aortic	–	–	–	–	7.8; (0.8); 50
Pulmonary	–	–	–	–	8.2; (0.8); 50
Heart diameter (mm)	133.6; (13.4); 50	136.7; (13.6); 50	141.9; (12.2); 50	142.6; (12.1); 50	–
Thoracic diameter (mm)	257; (22); 50	256.6; (21.6); 50	258.6; (21.1); 50	258.8; (21.3); 50	–
Cardiothoracic ratio	0.522; (0.057); 50	0.535; (0.058); 50	0.55; (0.049); 50	0.553; (0.049); 50	–
Heart weight (g)	–	–	–	–	472.7; (112.3); 50

Finally, the BIC analyses of the best two modalities (the venous phases for the CTR and the maximum cardiac diameter) to get the best correlation with the heart weight displayed the huge advantage to use the maximum cardiac diameter, instead of the CTR, on the venous phase (BIC = 22.5).

Discussion

CT angiography and cardiac magnetic resonance imaging (MRI) are the gold standard in clinical practice for coronary vessel and heart imaging, respectively [31–34]. Thanks to the development of the MPMCTA, the investigation of the CV system has become a routine tool also in forensic medicine. However, autopsy still remains the method of choice for CV measurements.

As mentioned above, these measurements determine if CV pathology exists. Indeed, they are important because an increased heart weight can be suggestive of hypertrophic cardiomyopathy, some valvular diseases, advanced stage of ischemic heart disease, pulmonary hypertension, and other chronic diseases. All of which should be carefully considered during autopsy and histological examination [29, 35, 36]. It is considered that measurements of the circumferences of valves can be useful for incompetence [16, 37]. An increase of aortic diameter suggests the most frequent aortic disease dominated by aneurysms of various types related to inflammatory or noninflammatory media degeneration [38, 39].

Moreover, in postmortem, it is impossible to assess the heart function because the echocardiography, the reference examination used for living, cannot be performed. Therefore, the CV measurements at autopsy are the only objective parameters of a pathological heart function.

However, the great importance of the PM changes does not allow an application of the clinical radiologic parameters and reference values [17–21]. For that reason, the necessity to find, thanks to MPMCTA, new radiological CV measurements that correlate with autopsy finding became an essential field of research in PM imaging.

For that reason, we decided to answer the following questions with this study: do radiological CV measurements performed on postmortem PMCT and MPMCTA correlate with

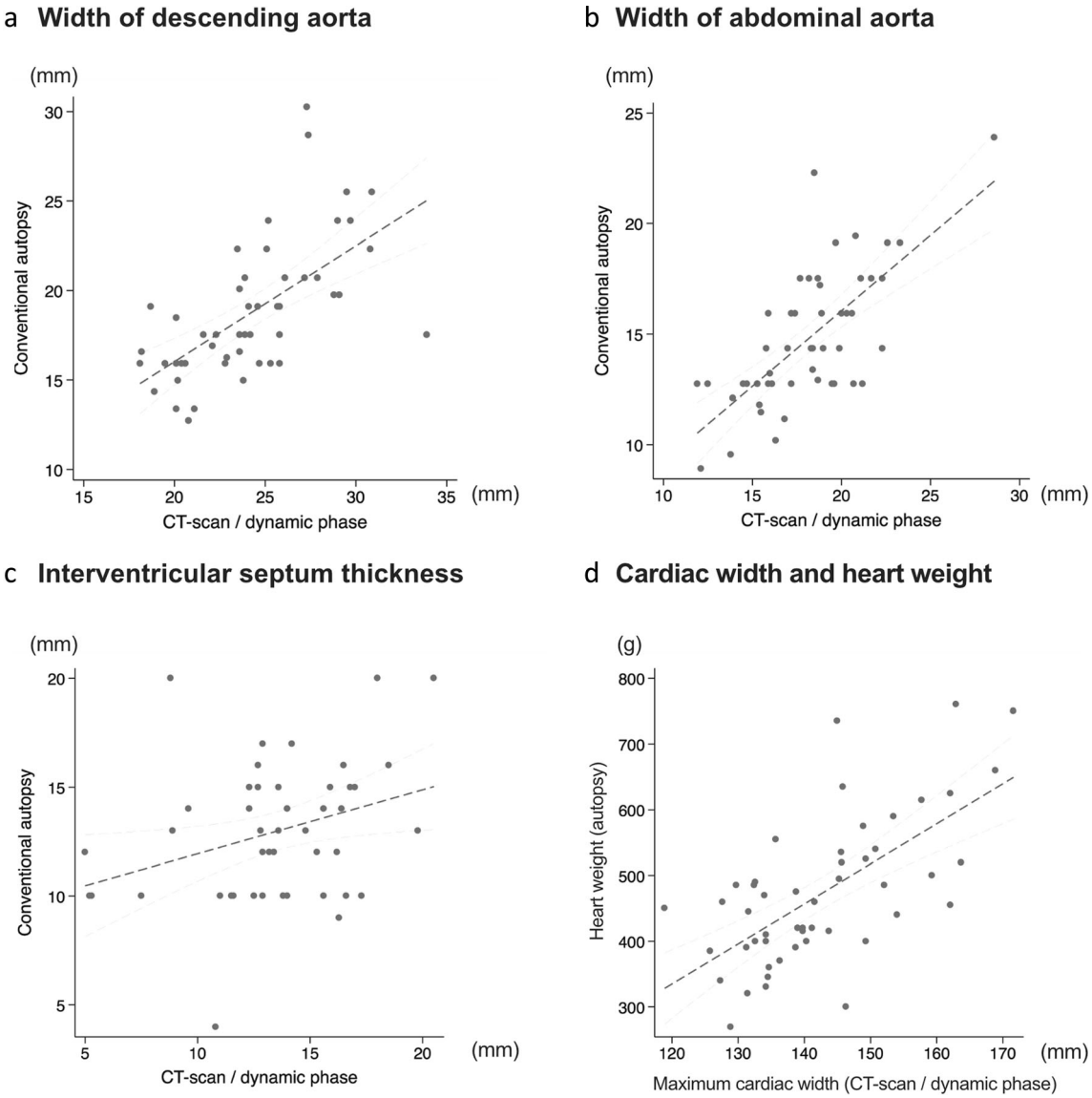

Fig. 6 Correlation between the measurements on the dynamic phases of the MPMCTA and at the autopsy. **a** Descending aorta. **b** Abdominal aorta. **c** Interventricular septum thickness. **d** Correlation between the maximal cardiac diameter on the dynamic phase of the MPMCTA and the heart weight at the autopsy

autopsy CV measurements and in which phase of the MPMCTA the best correlation can be obtained?

Our results show that the measurements of the descending and abdominal aortas in the dynamic phase exhibit the stronger correlation with the autopsy. Moreover, the BIC analyses display the importance to measure these vessels on the dynamic phase.

This first result is not surprising. Indeed, as proposed by the literature [3, 12, 25], unenhanced CT scan does not allow a good visualization of the CV system. Therefore, it is important to use contrast media to measure accurately the diameter of the aorta. A further important point is the usefulness of the dynamic phase. This latter allows a more effective filling of the vascular system to obtain images of greater quality, thus allowing to measure the diameter of the vessels [12]. In addition, the filling volume offsets the flattening by the surrounding tissue [12, 19]. Furthermore, although it is a well-known fact that the diameter of the aorta decrease after death [18, 19, 24], this effect is attenuated by the increasing diameter of the vessel caused by the injection of a lipophilic contrast media [8, 40].

Concerning the weak correlation between the heart walls' thicknesses on MPMCTA and at the autopsy, our results are quite surprising. Moreover, the BIC analysis did not show an advantage to perform the measurements of the heart walls and the interventricular septum on the dynamic phase.

In effect, CT scan is a poor technique to clearly visualize the cardiac soft tissue [4, 5, 22]. Therefore, it is difficult to

Table 4 Correlation between CV measurements at the CT-scan and the autopsy including a detailed comparison of measurements between the dynamic phase and the other phases of MPMCTA (native CT scan, arterial phase, and venous phase)

		Alternative phases		
	Dynamic phase R^{2a}; n	Native CT scan R^{2a}; n; BIC[b]	Arterial phase R^{2a}; n; BIC[b]	Venous phase R^{2a}; n; BIC[b]
Aortas				
Descending	0.382***; 50	0.265***; 50; 8.6	0.194**; 50; 13.2	0.332***; 50; 3.9
Abdominal	0.486***; 50	0.246***; 50; 19.2	0.311***; 50; 14.7	0.418***; 50; 6.2
Heart thicknesses				
Right ventricle	0.004; 50	–	<0.001; 31; 0.8	0.018; 49; −1.1
Left ventricle	0.070*; 43	–	0.126*; 34; 0.9	0.056; 41; 1.6
Interventricular septum	0.087*; 47	–	0.121*; 38; 3.3	0.100*; 46; −0.2

Linear regression test of significance, *$p < 0.05$; **$p < 0.01$; ***$p < 0.001$

[a] Adjusted R^2 using Mc Fadden's method

[b] Bayesian information criterion (BIC) corresponds to the difference of prediction ability of findings during conventional autopsy for alternative CT scan compared to the dynamic phase

measure the three thicknesses accurately. Also, an important pitfall of MPMCTA compared to clinical practice, is that both ECG-gated cardiac CT and cardiac MRI allow the measuring of the left ventricular wall thickness to be performed during the tele-diastolic phase of the cardiac cycle, while the myocardium is relaxed, thus avoiding an overestimation, due to the contracted cardiac muscles [32]. However, as proposed by Grabherr et al. [25], the high radio-opacity of the contrast media allows a better delineation of the inner walls in the heart cavities. Finally, as proposed by Okuma et al. [17], the CT scan did not allow a good distinction between the heart walls, the papillary muscles, and the epicardial fat. This latter causes an overestimation of the heart walls and the inter-ventricular septum at the MPMCT compared to the autopsy, where only the myocardium is measured, but not the trabecular muscles that cover the inner layer of the ventricle.

In order to explain the weak correlation between the measurements obtain at the MPMCTA and at the autopsy, we formulate some hypothesis. Firstly, although the long-axis views of the heart is the routine way to assess the heart wall thicknesses in our center, the latter could not be the method of choice to measure them. Secondly, the shorter range of the thickness measurements, compared to the aortas, could be more conclusive to cause a weak correlation with a slight variation in measurements. Thirdly, some individual differences related to the forensic pathologists in charge of the autopsy could explain this result too. Finally, we suppose that discrepancies in heart wall thickness most likely come from the difficulty of finding the same slice between imaging and autopsy. Septum thickness varies greatly, and the CT scan slice was done at a different location than the one created when opening the heart during the autopsy.

This study displays the fact that the long axis of the heart did not allow an accurate measurement of the thicknesses compared to the autopsy. To overcome this point, we can propose two possibilities. The first one consists in finding another measurement that better correlate with the ones obtained at the autopsy. The second one consists in measuring the heart wall on the MRI. This latter should allow a better visualization and demarcation of the soft tissues, as proposed by Aghayev et al. [22, 41].

With regard to the correlation between the cardiac valves measurements obtained at the autopsy and the heart cavities measured on CT scan, our results are slightly surprising. In effect, the statistical analysis showed no correlation. Furthermore, the BIC analysis did not display an advantage to carry out the heart cavity measurements on any phase of the MPMCTA.

In spite of the anatomical proximities and the pathological functioning [42–51] that urged our study to analyze the correlation between the right atrium and the tricuspid valve, the right ventricle and the pulmonary valve, the left atrium and the mitral valve, and the left ventricle and the aortic valve, our results did not display any correlation. This outcome could be explained by two hypotheses. Firstly, although the autopsy still remains the gold standard to measure the valve circumference, the heart cavity measurement on the CT scan undertook in accordance with our methodology could not be the best way to estimate these latter. Another measurement, such as the volume of the heart cavities, could be better correlated to the autopsy measurements. Secondly, the cases with a severe valvular incompetence and a dilatation of the valve annulus were treated with a prosthetic valve. Unfortunately, the latter had to be excluded from our study, in accordance with our methodology.

With respect to the correlation between the heart weight at the autopsy and the CTR just as the maximal cardiac diameter on the CT scan, our results were quite surprising. In fact, CTR can be measured reliably on the CT scan compared to the routine gold standard chest film [52, 53]. However, our results

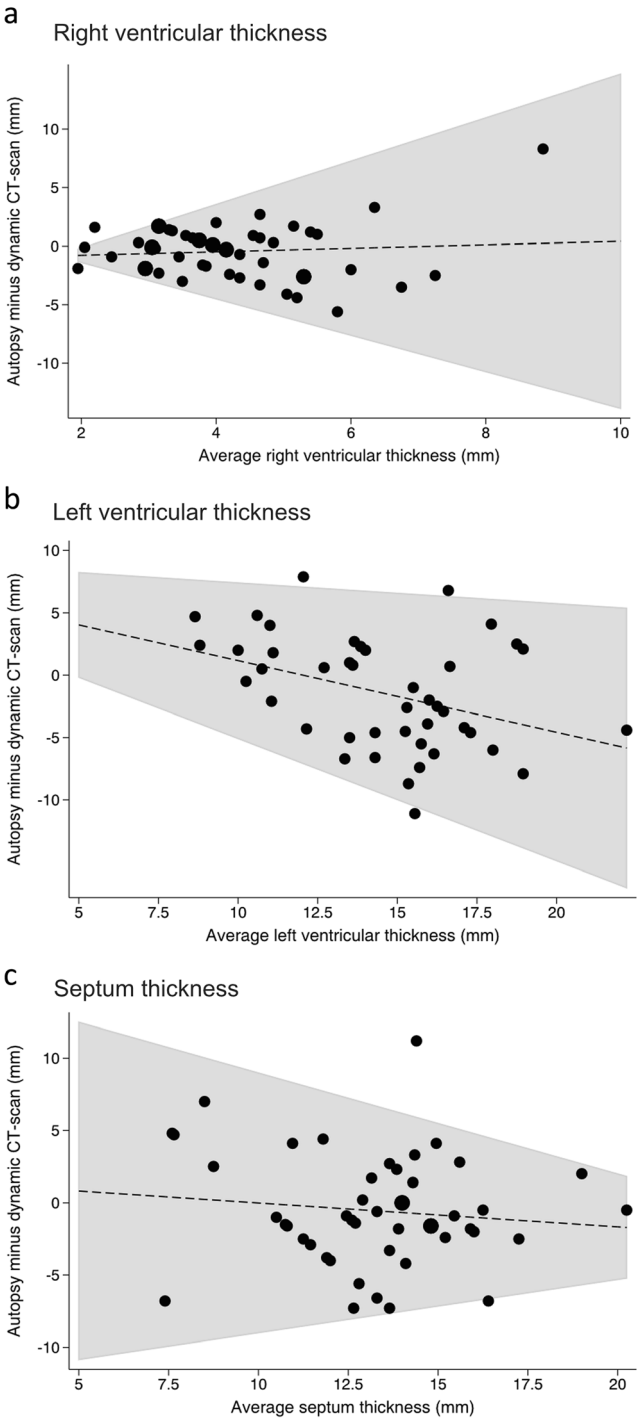

Fig. 7 Bland Altman plot comparing measures of heart thickness measures from dynamic phase of the CT scan and autopsy. *Dots* correspond to observed differences between measuring methods, *gray zone* corresponds to heteroscedasticity, and *dotted line* corresponds to the regression line of observed differences

display only a weak significant correlation on the venous and the dynamic phase of the CTR with the heart weight. In addition, the BIC analyses did not show any advantage to perform the measurements on any phase. This result is in agreement with Jotterand et al. [21] who did not display a significant correlation between the heart weight and the CTR on the native PM CT scan.

However, a good and significant correlation was found between the heart weight and the maximal cardiac diameter on the venous and the dynamic phase. Moreover, the BIC analyses display the great advantage to measure the latter on these two phases. This discovery is especially important due to the fact that the heart weight is a potentially key factor of cardiomyopathies [29]. This is why it is important to find a radiological measurement that accurately correlates with the heart weight obtained at the autopsy. Until today, the latter still remains the gold standard.

Nevertheless, our study highlights the usefulness of the MPMCTA, thanks to the venous and dynamic phase, to evaluate the heart weight. It proves the need to fill the heart cavities to perform a measurement that correlate significantly with the heart weight.

In summary, the results of our study show that only the measurement of the descending and abdominal aorta, which is regularly measured in autopsy, can be obtained by MPMCTA, especially on the dynamic phase in a comparable way to autopsy measurements. Furthermore, the heart weight measured at the autopsy correlates significantly with the maximal cardiac diameter obtained on the venous and the dynamic phases.

The other measurements such as the heart wall thicknesses, the heart cavities, and the CTR differ from the measurement obtained at the autopsy. This is why we need to define new reference values for the CV measurement on postmortem CT scan and MPMCTA that better estimate the values obtained at the autopsy, because the latter still remains the gold standard.

Limitations

Firstly, the retrospective design of this study did not allow us to include cases of important cardiovascular disease with clear signs of cardiac hypertrophy or valvular deficiencies, making correlations more difficult to detect. Secondly, this was an exploratory study; therefore, we relied on a convenient sample size for which we assumed to have enough power to test our hypothesis. Even if we did not report corrected *p* values for multiple testing, the observed correlation were strong enough to remain significant even after correction.

Finally, our observations do not extend to corpses in an advanced state of decomposition.

Conclusion

According to our knowledge, this is the first study that compares CV measurements between the native CT scan

Table 5 Correlation between the heart cavities at the CT scan and the cardiac valves at the autopsy including a detailed comparison of measurements between the dynamic phase and the other phases of MPMCTA (native CT scan, arterial phase, and venous phase)

		Alternative phases	
	Dynamic phase R^{2a}; n	Arterial phase R^{2a}; n; BIC[b]	Venous phase R^{2a}; n; BIC[b]
Mitral valve	<0.001; 49	<0.001; 49; 0.2	<0.001; 49; 0.4
Tricuspid valve	<0.001; 50	0.008; 50; −1.1	<0.001; 50; −0.1
Aortic valve	<0.001; 50	<0.001; 50; −0.01	<0.001; 50; 0.2
Pulmonary valve	0.027; 50	0.017; 50; 0.5	0.051; 50; −1.2

Linear regression test of significance, *$p < 0.05$; **$p < 0.01$; ***$p < 0.001$

[a] Adjusted R^2 using Mc Fadden's method

[b] Bayesian information criterion (BIC) corresponds to the difference of prediction ability of findings during conventional autopsy for alternative CT scan compared to the dynamic phase

Table 6 Correlation between the CTR or the cardiac diameter at the CT scan and the heart weight at the autopsy including a detailed comparison of measurements between the dynamic phase and the other phases of MPMCTA (native CT scan, arterial phase, and venous phase)

		Alternative phases		
	Dynamic phase R^{2a}; n	Native CT scan R^{2a}; n; BIC[b]	Arterial phase R^{2a}; n; BIC[b]	Venous phase R^{2a}; n; BIC[b]
CTR	0.075*; 50	0.044; 50; 1.6	0.044; 50; 1.6	0.09*; 50; −0.8
Cardiac diameter	0.418***; 50	0.262***; 50; 11.9	0.290***; 50; 9.9	0.421***; 50; −0.2

Linear regression test of significance *$p < 0.05$; **$p < 0.01$; ***$p < 0.001$

[a] Adjusted R^2 using Mc Fadden's method

[b] Bayesian information criterion (BIC) corresponds to the difference of prediction ability of findings during conventional autopsy for alternative CT scan compared to the dynamic phase

with the three phases of the MPMCTA and the autopsy. The results of the latter are promising on the possibility of measuring CV parameters obtained at the autopsy with the imaging, such as measuring the aorta and the cardiac wall thicknesses and estimating the heart weight and cardiac valve diameters though the maximal cardiac diameter and the heart cavities, respectively. However, as demonstrated by some inconclusive results, we need to carry out more studies on this field of research to allow the CV measurements on MPMCTA to become a routine tool in forensic imaging.

Compliance with ethical standards The following study was approved by the Cantonal Ethics Committees on research involving humans (CER-VD; No. 130/15).

Conflict of interest The authors declare that they have no conflict of interest.

References

1. Jackowski C, Persson A, Thali MJ (2008) Whole body postmortem angiography with a high viscosity contrast agent solution using poly ethylene glycol as contrast agent dissolver. J Forensic Sci 53: 465–468. doi:10.1111/j.1556-4029.2008.00673.x
2. Grabherr S, Djonov V, Yen K, Thali MJ, Dirnhofer R (2007) Postmortem angiography: review of former and current methods. AJR Am J Roentgenol 188:832–838. doi:10.2214/AJR.06.0787
3. Saunders SL, Morgan B, Raj V, Rutty GN (2011) Post-mortem computed tomography angiography: past, present and future. Forensic Sci Med Pathol 7:271–277. doi:10.1007/s12024-010-9208-3
4. Grabherr S, Grimm J, Dominguez A, Vanhaebost J, Mangin P (2014) Advances in post-mortem CT-angiography. Br J Radiol 87:20130488. doi:10.1259/bjr.20130488
5. Chevallier C, Doenz F, Vaucher P, Palmiere C, Dominguez A, Binaghi S, Mangin P, Grabherr S (2013) Postmortem computed tomography angiography vs. conventional autopsy: advantages and inconveniences of each method. Int J Legal Med 127:981–989. doi:10.1007/s00414-012-0814-3
6. Grabherr S, Grimm J, Heinemann A (2016) Atlas of postmortem angiography. Springer Int. doi:10.1007/978-3-319-28537-5
7. Saunders SL, Morgan B, Raj V, Robinson CE, Gn R (2011) Targeted post-mortem computed tomography cardiac angiography: proof of concept. Int J Legal Med 125:609–616. doi:10.1007/s00414-011-0559-4
8. Jackowski C, Sonnenschein M, Thali MJ, Aghayev E, von Allmen G, Yen K, Dirnhofer R, Vock P (2005) Virtopsy: postmortem minimally invasive angiography using cross section techniques—implementation and preliminary results. J Forensic Sci 50:1175–1186
9. Ross S, Spendlove D, Bolliger S, Christe A, Oesterhelweg L, Grabherr S, Thali MJ, Gygax E (2008) Postmortem whole-body CT angiography: evaluation of two contrast media solutions. AJR Am J Roentgenol 190:1380–1389. doi:10.2214/AJR.07.3082

10. Grabherr S, Grimm J, Baumann P, Mangin P (2015) Application of contrast media in post-mortem imaging (CT and MRI). Radiol Med 120:824–834. doi:10.1007/s11547-015-0532-2
11. Grabherr S, Gygax E, Sollberger B, Ross S, Oesterhelweg L, Bolliger S, Christe A, Djonov V, Thali MJ, Dirnhofer R (2008) Two-step postmortem angiography with a modified heart-lung machine: preliminary results. AJR Am J Roentgenol 190:345–351. doi:10.2214/AJR.07.2261
12. Grabherr S, Doenz F, Steger B, Dirnhofer R, Dominguez A, Sollberger B, Gygax E, Rizzo E, Chevallier C, Meuli R, Mangin P (2011) Multi-phase post-mortem CT angiography: development of a standardized protocol. Int J Legal Med 125:791–802. doi:10.1007/s00414-010-0526-5
13. Wichmann D, Heinemann A, Weinberg C, Vogel H, Hoepker WW, Grabherr S, Pueschel K, Kluge S (2014) Virtual autopsy with multiphase postmortem computed tomographic angiography versus traditional medical autopsy to investigate unexpected deaths of hospitalized patients: a cohort study. Ann Intern Med 160:534–541. doi:10.7326/M13-2211
14. Basso C, Burke M, Fornes P, Gallagher PJ, de Gouveia RH, Sheppard M, Thiene G, van der Wal A, Association for European Cardiovascular Pathology (2008) Guidelines for autopsy investigation of sudden cardiac death. Virchows Arch 452:11–18. doi:10.1007/s00428-007-0505-5
15. Maleszewski JJ, Lai CK, Veinot JP. (2016) Anatomic considerations and examination of cardiovascular specimens (excluding devices). In: Buja LM, Butany J, eds. Cardiovascular pathology, 4th edition. Elsevier. Pp. 1-56
16. Sheppard MN (2011) Practical cardiovascular pathology, 2nd edn. Oxford University Press, London
17. Okuma H, Gonoi W, Ishida M, Shintani Y, Takazawa Y, Fukayama M, Ohtomo K (2013) Heart wall is thicker on postmortem computed tomography than on antemortem [corrected] computed tomography: the first longitudinal study. PLoS One 8:e76026. doi:10.1371/journal.pone.0076026
18. Hyodoh H, Sato T, Onodera M, Washio H, Hasegawa T, Hatakenaka M (2012) Vascular measurement changes observed using postmortem computed tomography. Jpn J Radiol 30:840–845. doi:10.1007/s11604-012-0134-z
19. Takahashi N, Higuchi T, Hirose Y, Yamanouchi H, Takatsuka H, Funayama K (2013) Changes in aortic shape and diameters after death: comparison of early postmortem computed tomography with antemortem computed tomography. Forensic Sci Int 225:27–31. doi:10.1016/j.forsciint.2012.04.037
20. Shiotani S, Kohno M, Ohashi N, Yamazaki K, Nakayama H, Watanabe K, Itai Y (2003) Dilatation of the heart on postmortem computed tomography (PMCT): comparison with live CT. Radiat Med 21:29–35
21. Jotterand M, Doenz F, Grabherr S, Faouzi M, Boone S, Mangin P, Michaud K (2016) The cardiothoracic ratio on post-mortem computer tomography. Int J Legal Med. doi:10.1007/s00414-016-1328-1
22. Aghayev E, Sonnenschein M, Jackowski C, Thali M, Buck U, Yen K, Bolliger S, Dirnhofer R, Vock P (2006) Postmortem radiology of fatal hemorrhage: measurements of cross-sectional areas of major blood vessels and volumes of aorta and spleen on MDCT and volumes of heart chambers on MRI. AJR Am J Roentgenol 187:209–215. doi:10.2214/AJR.05.0222
23. Winklhofer S, Berger N, Ruder T, Elliott M, Stolzmann P, Thali M, Alkadhi H, Ampanozi G (2014) Cardiothoracic ratio in postmortem computed tomography: reliability and threshold for the diagnosis of cardiomegaly. Forensic Sci Med Pathol 10:44–49. doi:10.1007/s12024-013-9504-9
24. Shiotani S, Kohno M, Ohashi N, Yamazaki K, Nakayama H, Ito Y, Kaga K, Ebashi T, Itai Y (2002) Hyperattenuating aortic wall on postmortem computed tomography (PMCT). Radiat Med 20:201–206
25. Grabherr S, Hess A, Karolczak M, Thali MJ, Friess SD, Kalender WA, Dirnhofer R, Djonov V (2008) Angiofil-mediated visualization of the vascular system by microcomputed tomography: a feasibility study. Microsc Res Tech 71:551–556. doi:10.1002/jemt.20585
26. Lu MT, Ersoy H, Whitmore AG, Lipton MJ, Rybicki FJ (2007) Reformatted four-chamber and short-Axis views of the heart using thin section (≤2mm) MDCT images. Acad Radiol 14:1108–1112. doi:10.1016/j.acra.2007.05.019
27. Brinkmann B (1999) Harmonization of medico-legal autopsy rules. Committee of Ministers. Council of Europe. Int J Legal Med 113:1–14
28. Société Suisse de Médecine Légale (2007). Swiss Principles and Rules for Medico-Legal Autopsy https://www.sgrm.ch/inhalte/Forensische-Medizin/Durchfuehrung_Rechtsmed_Obduktion_01.pdf. Accessed 20 December 2016
29. Vanhaebost J, Faouzi M, Mangin P, Michaud K (2014) New reference tables and user-friendly internet application for predicted heart weights. Int J Legal Med 128:615–620. doi:10.1007/s00414-013-0958-9
30. Raftery AE (1995) Bayesian model selection in social research. Sociol Methodol 25:111–163. doi:10.2307/271063
31. Guthaner DF, Wexler L, Harell G (1979) CT demonstration of cardiac structures. AJR Am J Roentgenol 133:75–81. doi:10.2214/ajr.133.1.75
32. Roberts WT, Bax JJ, Davies LC (2008) Cardiac CT and CT coronary angiography: technology and application. Heart 94:781–792. doi:10.1136/hrt.2007.116392
33. Kumamaru KK, Hoppel BE, Mather RT, Rybicki FJ (2010) CT angiography: current technology and clinical use. Radiol Clin N Am 48(213–35):vii. doi:10.1016/j.rcl.2010.02.006
34. Rubin GD, Leipsic J, Joseph Schoepf U, Fleischmann D, Napel S (2014) CT angiography after 20 years: a transformation in cardiovascular disease characterization continues to advance. Radiology 271:633–652. doi:10.1148/radiol.14132232
35. Kitzman DW, Scholz DG, Hagen PT, Ilstrup DM, Edwards WD (1988) Age-related changes in normal human hearts during the first 10 decades of life. Part II (maturity): a quantitative anatomic study of 765 specimens from subjects 20 to 99 years old. Mayo Clin Proc 63:137–146
36. de la Grandmaison GL, Clairand I, Durigon M (2001) Organ weight in 684 adult autopsies: new tables for a Caucasoid population. Forensic Sci Int 119:149–154. doi:10.1016/s0379-0738(00)00401-1
37. Burke AP, Tavora F (2010) Practical cardiovascular pathology. Lippincott Williams and Wilkins, Philadelphia
38. Halushka MK, Angelini A, Bartoloni G et al (2016) Consensus statement on surgical pathology of the aorta from the Society for Cardiovascular Pathology and the Association For European Cardiovascular Pathology: II. Noninflammatory degenerative diseases - nomenclature and diagnostic criteria. Cardiovasc Pathol 25:247–257. doi:10.1016/j.carpath.2016.03.002
39. Stone JR, Bruneval P, Angelini A et al (2015) Consensus statement on surgical pathology of the aorta from the Society for Cardiovascular Pathology and the Association for European Cardiovascular Pathology: I. Inflammatory diseases. Cardiovasc Pathol 24:267–278. doi:10.1016/j.carpath.2015.05.001
40. Frik W, Persch WF (1969) The effect of contrast media type on the vascular caliber in experimental angiography. Fortschr Geb Röntgenstr Nuklearmed 111:620–629
41. Ampanozi G, Hatch GM, Flach PM, Thali MJ, Ruder TD (2015) Postmortem magnetic resonance imaging: reproducing typical autopsy heart measurements. Legal Med 17:493–498. doi:10.1016/j.legalmed.2015.10.008

42. Ariyarajah V, Soni A, Morris A (2008) Giant right atrium in an adult. Echocardiography 25:1121–1123. doi:10.1111/j.1540-8175.2008.00742.x
43. Kelesidis T, Maysky M, Kelesidis I (2010) Giant right atrium with severe pulmonary hypertension. Can Med Assoc J 182:E147–E147. doi:10.1503/cmaj.090671
44. Thompson SI, Vieweg WV, Iacovoni VE, Alpert JS, Haggan AD (1978) Idiopathic enlargement of the right atrium: report of three cases. Maryl Med J 27
45. Anzouan-Kacou JB, Konin C, Coulibaly I, N'guetta R, Adoubi A, Soya E, Boka B (2011) Unusual giant right atrium in rheumatic mitral stenosis and tricuspid insufficiency. Case Rep Cardiol 2011:1–4. doi:10.1155/2011/762873
46. Biscione C, Sergnese O, Forleo GB, Costantino MF, Andreotta P, Romeo F (2013) Giant left atrium 30years after surgical mitral valve replacement: an assessment of conservative therapy. Int J Cardiol 166:e6–e8. doi:10.1016/j.ijcard.2012.12.079
47. Chick JFB, Sheehan SE, Miller JD, Bair RJ, Madan R (2013) Giant left atrium in rheumatic heart disease: the classic signs of left atrial enlargement. J Emerg Med 44:393–394. doi:10.1016/j.jemermed.2012.11.066
48. Mainwaring RD, Pirolli T, Punn R, Hanley FL (2012) Late repair of the native pulmonary valve in patients with pulmonary insufficiency after surgery for tetralogy of fallot. Ann Thorac Surg 93:677–679. doi:10.1016/j.athoracsur.2011.09.016
49. Mercer-Rosa L, Ingall E, Zhang X et al (2015) The impact of pulmonary insufficiency on the right ventricle: a comparison of isolated valvar pulmonary stenosis and tetralogy of Fallot. Pediatr Cardiol 36:796–801. doi:10.1007/s00246-014-1087-z
50. Gaasch WH, Carroll JD, Levine HJ, Criscitiello MG (1983) Chronic aortic regurgitation: prognostic value of left ventricular end-systolic dimension and end-diastolic radius/thickness ratio. J Am Coll Cardiol 1:775–782. doi:10.1016/S0735-1097(83)80190-9
51. Fioretti P, Roelandt J, Sclavo M, Domenicucci S, Haalebos M, Bos E, Hugenholtz PG (1985) Postoperative regression of left ventricular dimensions in aortic insufficiency: a long-term echocardiographic study. J Am Coll Cardiol 5:856–861. doi:10.1016/S0735-1097(85)80423-X
52. Miller JA, Singer A, Hinrichs C, Contractor S, Doddakashi S (1999) Cardiac dimensions derived from helical CT: correlation with plain film radiography. Internet J Radiol 1
53. Gollub MJ, Panu N, Delaney H, Sohn M, Zheng J, Moskowitz CS, Rademaker J, Liu J (2012) Shall we report cardiomegaly at routine computed tomography of the chest? J Comput Assist Tomogr 36:67–71. doi:10.1097/RCT.0b013e318241e585